ACS OMEGA

http://pubs.acs.org/journal/acsodf

Article

Self-Assembly of Ag_2S Colloidal Nanoparticles Stabilized by MPS in Water Solution

Svetlana V. Rempel,* Yulia V. Kuznetsova, and Andrey A. Rempel

Cite This: *ACS Omega* 2020, 5, 16826−16832

Read Online

ACCESS | Metrics & More | Article Recommendations

ABSTRACT: Self-assembly of colloidal Ag_2S nanoparticles (NPs) was studied in the presence of (3-mercaptopropyl)trimethoxysilane (MPS). Solutions with different molar ratios of Ag_2S/MPS were prepared. The appearance of nano- and microtubes was detected. Self-organized NPs were studied with optical microscopy, scanning electron microscopy (SEM), energy-dispersive X-ray spectroscopy (EDX), and high-resolution transmission electron microscopy (HRTEM). Silicon nuclear magnetic resonance spectroscopy (^{29}Si NMR) was used to study polycondensation of MPS molecules. Geometrical parameters of the nano- and microtubes depended on the molar ratio of Ag_2S/MPS. The scheme and mechanism of self-assembly of Ag_2S NPs in nanotubes in the presence of MPS were proposed. The effect of MPS on the preservation of the initial stoichiometry of Ag_2S NPs was discussed.

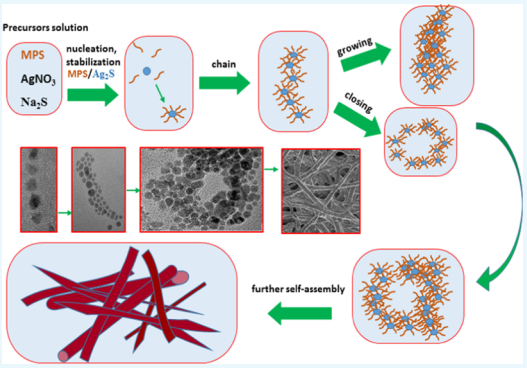

INTRODUCTION

The ability of nanoparticles (NPs) to self-assemble into superstructures under certain conditions is promising to design novel optical, catalytic, and magnetic devices, as well as to be used in medicine, pharmaceutics, and industrial processes. A new concept in designing a wide range of materials has appeared recently, which is called nanoarchitectonics. Self-assembly processes play a crucial role in this concept. Numerous complex mechanisms and a comprehensive approach are necessary for target architectures. Thus, self-assembly is currently one of the key topics in physics, chemistry, and mathematics.[1−7]

For NPs to be successfully used, they should be placed into a matrix or be stabilized with inorganic/organic materials. Organic ligands play an important role not only in the stabilization of inorganic NPs but also in the formation of two- and three-dimensional self-organized assemblies of NPs in ref 4. For medicine and biology, of interest are self-assembled structures based on inorganic NPs with biocompatible/bioactive organic molecules;[8−12] for example, nanomaterials based on self-assembly of charged polysaccharides, namely, chitosan and alginate, onto inorganic NPs can be used for efficient disinfection and microbial control. A promising material that can be used to stabilize and form target architectures is (3-mercaptopropyl)trimethoxysilane (MPS). The studies in refs 13−15 report about the assembly of mono- and two-dimensional (2D) structures based on MPS onto which different agents are mobilized to create immunosensors.

Silver sulfide (Ag_2S) NPs have attracted much attention due to their potential applications in photoconductors, solar cells, near-infrared photodetectors, biology, medicine, etc.[16−28] Under certain conditions, Ag_2S NPs are also capable of self-assembly.[29−31] In ref 25, it was shown that Ag_2S nanowires can be utilized as a catalyst for the electrochemical CO_2 reduction reaction.

Thus, to develop nanoarchitectures of novel materials, it is interesting to consider self-assembly processes in the Ag_2S/MPS system. In ref 32, a simple one-step synthesis of Ag_2S NPs in water solution with MPS as capping molecules was reported. The aim of the present study was to investigate the effects of different concentrations of MPS on self-assembly of Ag_2S colloidal NPs.

RESULTS AND DISCUSSION

The hydrodynamic diameter of NPs in solution was studied right after synthesis, 1 day later, and then 14 days after the synthesis (Table 1).

Immediately after the synthesis, the hydrodynamic radius of NPs was about 60 nm for all concentrations. The average NP diameter in the solution with the least concentration changed insignificantly with time; as the MPS concentration increased, the NP diameter increased almost 2-fold, and an additional fraction of micrometer-sized agglomerates appeared. The

Received: April 30, 2020
Accepted: June 18, 2020
Published: July 2, 2020

https://dx.doi.org/10.1021/acsomega.0c01994
ACS Omega 2020, 5, 16826−16832

Table 1. Hydrodynamic Diameter of Ag_2S NPs versus Ag_2S/MPS Molar Ratio and Time

		D_h, nm		
sample	Ag_2S/MPS molar ratio	0 days	1 day	14 days
Ag_2S–MPS 0.25	1:0.25	67 ± 24	81 ± 25	83 ± 27
Ag_2S–MPS 0.5	1:0.5	66 ± 21	68 ± 21	104 ± 24 (96%) 1670 ± 1000 (4%)
Ag_2S–MPS 1	1:1	58 ± 20	80 ± 26	137 ± 28 (90%) 928 ± 250 (10%)

samples with the maximal concentration of MPS contained particles with the maximal hydrodynamic diameter. This occurred due to MPS condensation.

Analysis of the obtained values and NP size distribution (Figure 1) allows concluding that at the initial stage MPS-

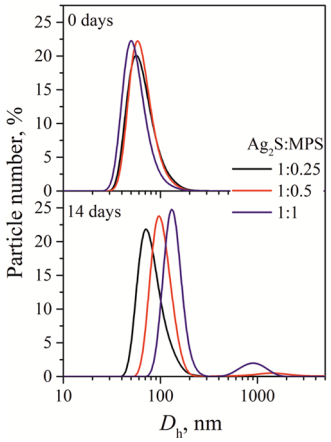

Figure 1. Number size distribution of Ag_2S NPs in water solution stabilized with different concentrations of MPS.

stabilized Ag_2S NPs are formed, and then they grow. It is reasonable to hypothesize that MPS plays an important role in increasing the NP size with time.

The optical properties of colloidal solutions after synthesis have been studied. Figure 2 presents the UV–vis–NIR optical

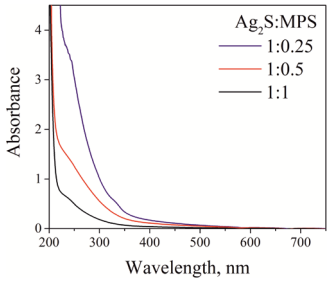

Figure 2. Optical absorption of aqueous solution that contains Ag_2S NPs covered by MPS.

absorption spectrum of the colloidal solution after synthesis that contains Ag_2S NPs covered by MPS. The colloidal Ag_2S absorption spectra in the 230–1250 nm region are represented by curves monotonically rising toward the short-wave side. An intensive increase in absorption, which starts at about 400 nm, is detected for all samples. Increasing the MPS concentration by increasing the MPS to Ag_2S ratio from 0.25 up to 1 results in decreasing optical absorption, which indicates the sedimentation of NPs due to agglomeration.

Silicon nuclear magnetic resonance spectroscopy (^{29}Si NMR) was used to establish the state of stabilizer molecules (monomers, hydrolyzed monomers, dimers, and short or long polymers) and to clarify the formation of agglomerates of Ag_2S NPs stabilized by MPS. ^{29}Si NMR spectra were obtained on the following samples: MPS (initial chemical reagent), MPS in alcohol, MPS in aqueous alcoholic solution, and an aqueous solution of Ag_2S NP stabilized by MPS.

The MPS monomer has one line in the ^{29}Si NMR spectrum with a chemical shift of about −42.506 ppm. After addition of alcohol, hydrolysis of MPS molecules begins, which leads to a change in the chemical shift to −40.07...39.95 ppm. At the same time, there is a signal from the nonhydrolyzed monomer MPS, however, with a shift of −41.7 ppm, which indicates incomplete hydrolysis during the measurement (Figure 3).

The difference from the value of the initial MPS (which coincides with that in the published data) can be caused by the solvent used (chloroform-*d*). The appearance of a line in the region of −48.5...−49.5 ppm indicates the formation of dimers. A weak signal in the region of −55...−80 ppm indicates the beginning of the process of polycondensation and the formation of polymer chains. At the same time, even after 14 h after the addition of water, a signal of −39.95 ppm is present, which may be associated with a small amount of water, which is sufficient for the hydrolysis of MPS but not enough for complete condensation and polycondensation of molecules. The signal at −50.84 ppm after the addition of water requires further analysis.

No signal was detected on the sample with Ag_2S NPs even after 30 h of collecting the statistics. This is due to a low concentration of MPS used for stabilization. The work on the synthesis of a stable sample with a higher concentration of MPS is underway.

After the obtained solutions were kept under normal conditions for one month, all of the samples exhibited changes in the form of precipitates or bulk suspension. The precipitate and the solution were examined using optical microscopy, scanning electron microscopy (SEM), energy-dispersive X-ray spectroscopy (EDX), and HRTEM methods.

In the sample with the initial Ag_2S/MPS ratio equal to 1:0.25, a dark precipitate was found at the bottom of the vessel. When agitated, the particles were distributed in the solution, but, at the same time, they seemed partly bound to each other. While investigating the precipitate by the HRTEM method, agglomerates with a dendritelike shape and rounded particles 2–20 nm in diameter were detected. All NPs were enclosed in an organic matrix. According to the measured interplanar spacing, large particles can be related to Ag_2S, and some smaller particles, to Ag (Figure 4). More often, especially in solution, thin chains of NPs connected with each other were observed. The agglomerates represented a cluster of such chains.

https://dx.doi.org/10.1021/acsomega.0c01994
ACS Omega 2020, 5, 16826–16832

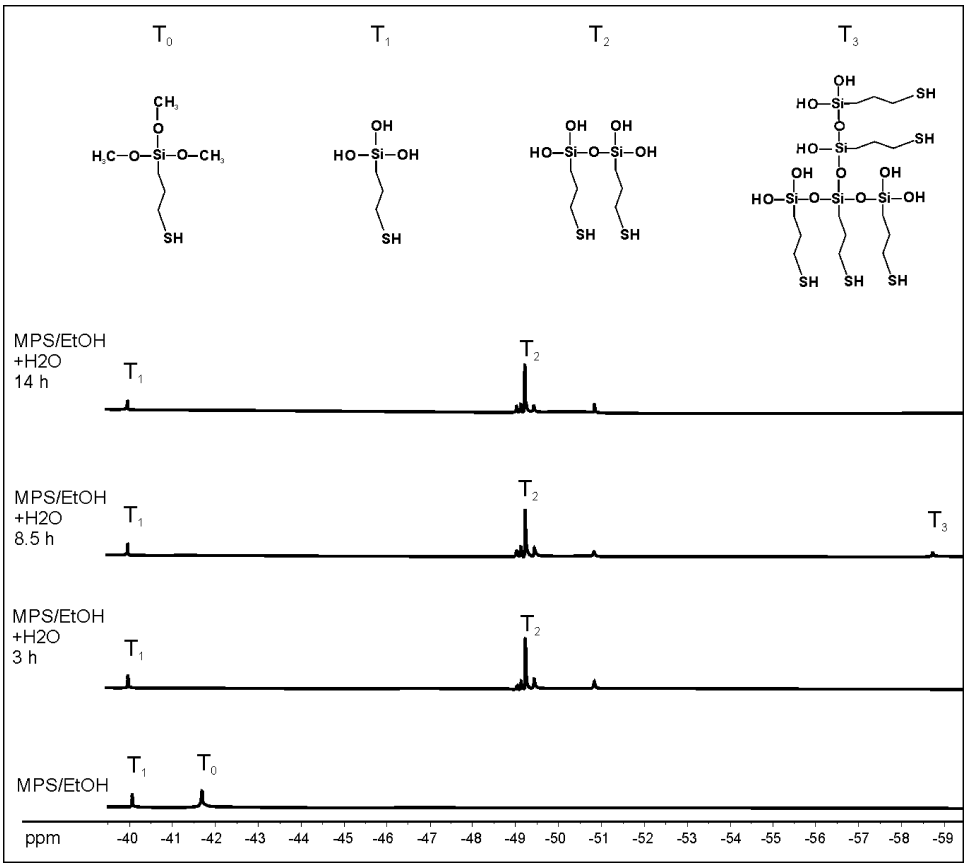

Figure 3. ^{29}Si NMR spectroscopy of MPS molecules in ethanol (MPS/EtOH) and in ethanol with water (MPS/EtOH + H_2O) after 3, 8.5, and 14 h. T_n shows the degree of hydrolysis and condensation of MPS molecules and their association through siloxane bonds (Si−O−Si). T_0, T_1, T_2, and T_3 represent MPS monomers, hydrolyzed monomers, dimers, and short polymer chains, respectively.

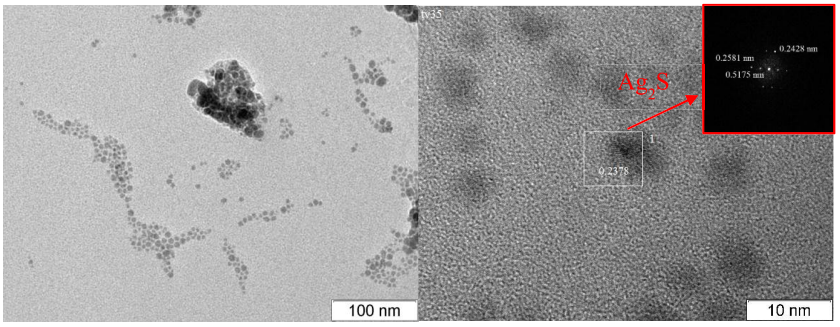

Figure 4. High-resolution transmission electron microscopy (HRTEM) images of the chains from the Ag_2S/MPS precipitate and solution (Ag_2S/MPS molar ratio 1:0.25).

At the Ag_2S/MPS ratio of 1:0.5, we also observed a precipitate at the bottom of the vessel, and transparent light brown conical formations were attached to the surface of the vessel (Figure 5a). Analysis of the precipitate using optical microscopy and SEM methods revealed hollow tubes with a diameter of about 1.5 μm. It is not possible to find the length of the tubes because they are interlaced into a loose ball. From the results of the analysis using the EDX method, it can be concluded that the tubes consist of Ag_2S and MPS (Figure 5).

Analysis of the precipitate with the HRTEM method revealed that the phase composition is analogous to that in the previous case. The agglomerates represent a cellular structure consisting of large chains; some chains, preserving a curved form, become thicker and contain more NPs than in the sample with the 1:0.25 ratio (Figure 6). In addition, fragments of tubes were observed at whose boundaries Ag_2S NPs were accumulated. The tubes were about 20 nm thick.

When the ratio of the initial Ag_2S/MPS components was 1:1, a suspended porous formation of interlaced light brown tubes was observed after a month. When a large amount of solution was synthesized at the same ratios of components, a suspended cloud of greater size was formed (Figure 7).

The results of the analysis of the samples with the HRTEM method demonstrated a developed matrix. Tubes with a diameter of 200−250 nm and a wall thickness of ∼20 nm were clearly observed. A matrix with individual NPs was located between the tubes. As in the previous cases, NPs of metallic Ag can be observed along with Ag_2S NPs. Large (to 50 nm) and

https://dx.doi.org/10.1021/acsomega.0c01994
ACS Omega 2020, 5, 16826−16832

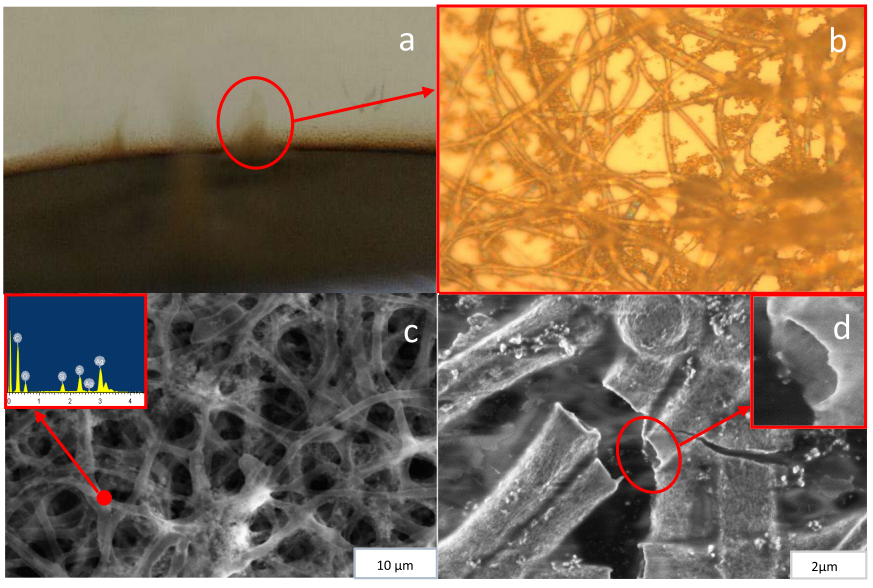

Figure 5. Optical images (a, b) and SEM images (c, d) of microtubes from the precipitate (Ag_2S/MPS molar ratio 1:0.5). The inset of (c) is EDX of the microtubes.

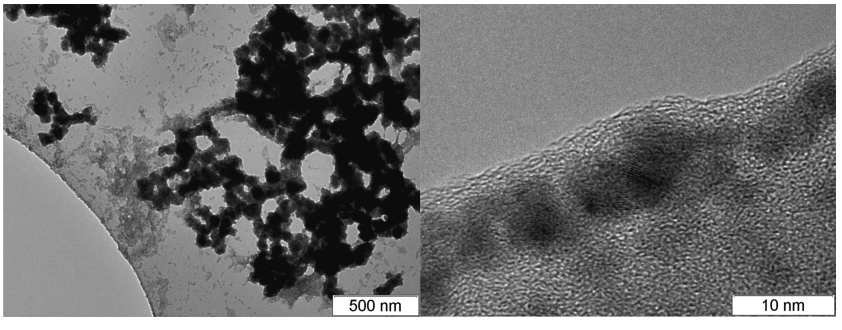

Figure 6. HRTEM images of the Ag_2S/MPS precipitate (Ag_2S/MPS molar ratio 1:0.5).

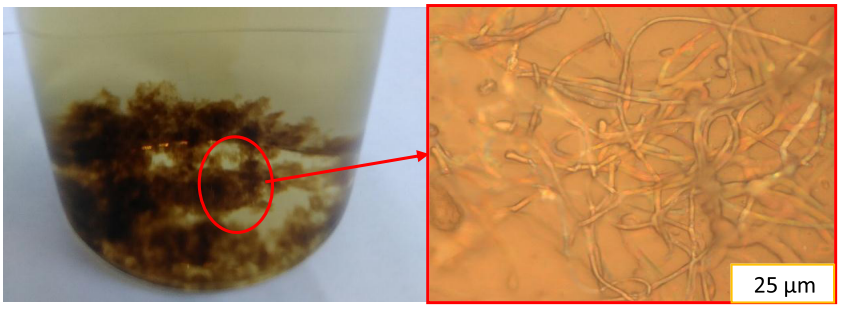

Figure 7. Optical image of the Ag_2S/MPS precipitate (Ag_2S/MPS molar ratio 1:1).

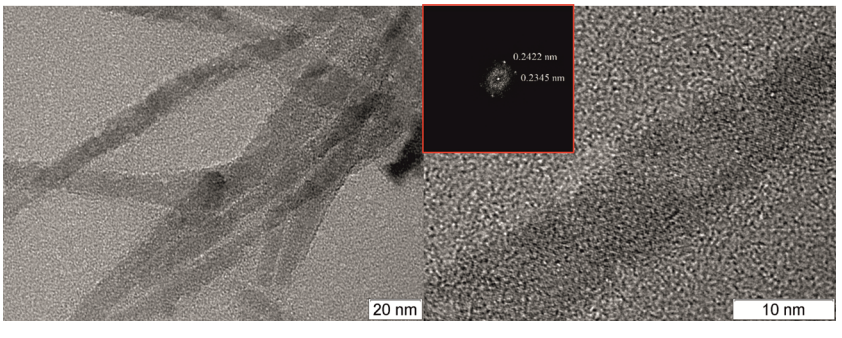

Figure 8. HRTEM images of the nanocores (Ag_2S/MPS molar ratio 1:1).

https://dx.doi.org/10.1021/acsomega.0c01994
ACS Omega 2020, 5, 16826−16832

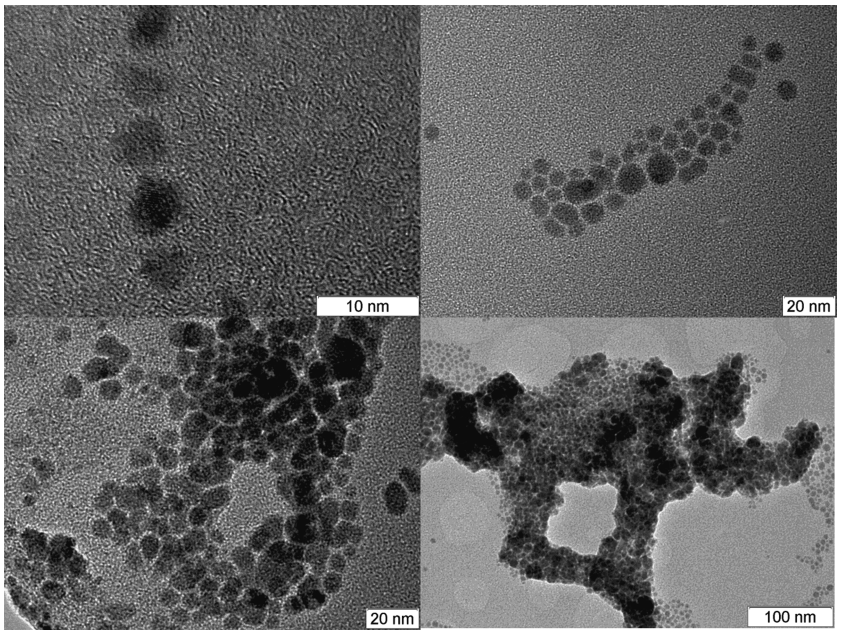

Figure 9. Schematic morphology evolution of nanotubes with HRTEM images.

smaller (3−20 nm) NPs of both fractions may consist of smaller crystallites. The content of metallic silver was insignificant, since it was not detected by X-ray photoelectron diffraction (XPD) analysis of the precipitates. Along with small chains, the solution contained nanorods of Ag_2S (10 nm thick and up to 300 nm long), which were modified under the action of an electron beam (Figure 8).

Thus, self-assembly of NPs into tubes was found in the presence of MPS. The thickness of the tube walls is about 20 nm, and the diameter depends on the initial content of MPS and is 200−300 nm; however, it can reach as much as 1.5 μm. The NPs of the dispersed phase are incorporated into the matrix. An increase in the MPS content leads to the formation of loose balls consisting of tubes of indefinite length. At the maximal concentration of MPS, Ag_2S nanorods are also detected in the solution. The modeling performed in ref 33 on the basis of the concepts of the DLVO (Derjaguin−Landau−Verwey−Overbeek) theory of aggregate stability of lyophobic disperse systems shows that individual NPs are united into chains due to the synchronous action of van der Waals and electrostatic forces. The chains are capable of uniting into tubular structures with time.

Thus, the chain structures consisting of MPS and NPs play a key role in the subsequent formation of microtubes. Increasing the relative content of MPS promotes the growth of such chains in length and width.

Based on the studies performed, it is possible to represent a scheme of the process of self-assembly of Ag_2S NPs in the presence of MPS (Figure 9).

At the moment right after synthesis, Ag_2S NPs stabilized by MPS are formed, and these NPs are about 60 nm in hydrodynamic diameter. Then, in the course of time, the particles grow due to their incorporation into chains and increase in their lateral dimensions as a result of polycondensation of MPS. In 14 days, the size of the main fraction becomes as much as 83, 104, and 137 nm for the ratios 1:0.25, 1:0.5, and 1:1, respectively. The size of the main fraction grows with increasing initial content of MPS. The process of polycondensation of MPS continues in the subsequent periods and leads to the formation of self-assembled structures in the form of hollow tubes Ag_2S/MPS and Ag nanorods. At the Ag_2S/MPS ratio of 1:1, the nanotubes become 1.5 μm in diameter, and clusters of nanotubes continue to exist for a long time in the solution in the form of a loose suspension until complete evaporation of the solvent. The mechanism of formation of nanorods in the presence of MPS requires further research on Ag_2S.

One more feature connected with the presence of MPS is noteworthy. Silver sulfide is prone to nonstoichiometry even in the low-temperature α-Ag_2S monoclinic phase,[34] which results in the $Ag_{2-x}S$ compound and the appearance of defects. The main defects are interstitial silver ions (I_{Ag}), sulfur vacancies (V_S), and substitutional defects (S_{Ag}). Owing to such a structure, Ag_2S NPs are easily reduced to Ag under different external actions. The presence of Ag NPs in colloidal solutions of Ag_2S with different stabilizers is a problem if it is necessary to produce a monophase material. Organic stabilizers, for example, sodium citrate $Na_3C_6H_5O_7$, lead to a considerable reduction of silver sulfide to pure silver.[28,35] Ag NPs were found in the examined samples with the use of the HRTEM method, while metallic Ag was not detected using the XPD method. The content of Ag may be below the sensitivity of this method. On the whole, the presence of metallic Ag was insignificant. Under the action of an electron beam, Ag_2S nanorods were modified as described in an earlier work.[27] The rounded NPs enclosed into the MPS matrix remained stable. Thus, the MPS shell protects the Ag_2S NPs from reduction to metallic Ag much better under the action of external factors, that is, it contributes to the preservation of initial stoichiometry.

CONCLUSIONS

The effect of MPS on the processes of stabilization and self-assembly of Ag_2S NPs in aqueous colloidal solutions at the initial point of time and in long-term investigations was considered in this work. A scheme of nanotube formation was proposed. At the first stage after synthesis, Ag_2S NPs covered with an MPS shell are formed. When the relative content of

https://dx.doi.org/10.1021/acsomega.0c01994
ACS Omega 2020, 5, 16826−16832

MPS and the concentration of Ag_2S/MPS increase due to polycondensation of MPS molecules, the process of self-assembly leads to the formation of microtubes from 200 nm to 1.5 μm in size, with a wall thickness of about 20 nm and indefinite length. These microtubes are interlaced into a ball. MPS plays a key role in the self-assembly. By varying the relative concentration of MPS it is possible to control the tube size. At the maximal concentration of MPS, Ag_2S nanorods are also observed in the solution. The MPS matrix protects Ag_2S NPs from the action of radiation, electron beam, and time factor. The results of the study of the self-assembly in the Ag_2S/MPS system can be useful for the development of nanoarchitectonics of novel functional materials.

MATERIALS AND METHODS

3-Mercaptopropyl-trimethoxysilane ($HSC_3H_6Si(OCH_3)_3$, >95%), sodium sulfide (Na_2S) from Sigma Aldrich, ethanol (EtOH), and silver nitrate ($AgNO_3$) from the domestic market were used. All of the chemicals were of analytical grade (ACS) and were used without further purification. Distilled water was used to prepare the sample. Ag_2S NPs were synthesized in a water solution by using the chemical condensation technique based on the exchange reaction between $AgNO_3$ and Na_2S. The overall molecular equation for the formation of the disperse phase of Ag_2S colloid solution can be written as follows

$$2AgNO_3 + Na_2S = (Ag_2S)_{NPs} + 2NaNO_3$$

Initial solutions of 1.25 mM $AgNO_3$ and 0.625 mM Na_2S were mixed in equal volumes to maintain the stoichiometric Ag-to-S ratio to be 2 to 1 under red lighting at ambient temperature (T_{at}) with the immediate addition of MPS solution in ethanol to prevent agglomeration and sedimentation of NPs. Sonication was carried out in an ultrasonic bath for 10 min to ensure the homogeneity and to complete the consumption of the reagents. The details of the synthesis procedure are presented in ref 29. It was found that an increase in the MPS content in the Ag_2S/MPS ratio to more than 1:1 results in agglomeration and precipitation. In contrast to ref 29, the MPS to Ag_2S NP molar ratios of 0.25, 0.5, and 1 were used in the experiments to study the effect of the stabilizing agent in the present work.

The hydrodynamic diameter, D_h, and number size distribution of Ag_2S NPs in the solution were measured using dynamic light scattering on a Zetasizer Nano ZS facility (Malvern Panalytical Ltd.) at 25 °C and a wavelength of 633 nm. All of the measurements were repeated three times for good statistics of the results. UV−vis−NIR optical characterization of the synthesized Ag_2S−MPS solutions was carried out using an FS5 spectrofluorometer (Edinburgh Instruments) at ambient temperature in the wavelength range from 230 to 1250 nm. Optical images were obtained by using a Leica 2500M DM microscope (Carl Zeiss). The images and EDX of the synthesized samples were obtained on a SIGMA VP (Carl Zeiss) scanning electron microscope (SEM) under high vacuum using an InLens detector.

HRTEM images of the synthesized Ag_2S−MPS solutions were recorded on a JEOL JEM-2010. The colloidal solutions of Ag_2S NPs were dropped on a copper grid and dried in air at room temperature for examination. The phase components were identified with fast Fourier transformation (FFT) of the HRTEM images. An X-ray diffraction analysis (XRD) study of the precipitate was performed on a STADI-P diffractometer (STOE, Germany). A silicon nuclear magnetic resonance (^{29}Si NMR) study of the MPS behavior in solution was performed on a Bruker Advance Neo 600 Spectrometer at 119 MHz at 298 K. Tetramethylsilane $Si(CH_3)_4$ (tetramethylsilane (TMS), 0 ppm) as the reference and chloroform-*d* (CDC13) as the solvent were used. For ^{29}Si NMR experiments, MPS concentrations of 3.15 g/L in a solution without NPs and 0.016 mg/L in a solution with NPs were used.

AUTHOR INFORMATION

Corresponding Author

Svetlana V. Rempel − *Institute of Solid State Chemistry, Ural Branch of the Russian Academy of Sciences, 620990 Ekaterinburg, Russia; Ural Federal University, 620002 Ekaterinburg, Russia;* orcid.org/0000-0002-8747-6719; Email: svetlana_rempel@ihim.uran.ru; Fax: +7 343 374 4495

Authors

Yulia V. Kuznetsova − *Institute of Solid State Chemistry, Ural Branch of the Russian Academy of Sciences, 620990 Ekaterinburg, Russia*

Andrey A. Rempel − *Institute of Solid State Chemistry, Ural Branch of the Russian Academy of Sciences, 620990 Ekaterinburg, Russia; Ural Federal University, 620002 Ekaterinburg, Russia; Institute of Metallurgy, Ural Branch of the Russian Academy of Sciences, 620016 Ekaterinburg, Russia*

Complete contact information is available at: https://pubs.acs.org/10.1021/acsomega.0c01994

Notes

The authors declare no competing financial interest.

ACKNOWLEDGMENTS

The authors are grateful to E. Y. Gerasimov, O. S. Eltsov, and I. D. Popov for their assistance. This work was supported by the RSF [project no. 19-73-20012].

REFERENCES

(1) Ghosh, S. K.; Böker, A. Self-Assembly of NP in 2D and 3D: Recent Advances and Future Trends. *Macromol. Chem. Phys.* **2019**, *220*, No. 1900196.

(2) Ariga, K.; Minami, K.; Ebara, M.; et al. What are the emerging concepts and challenges in NANO? Nanoarchitectonics, hand-operating nanotechnology and mechanobiology. *Polym. J.* **2016**, *48*, 371−389.

(3) Ariga, K.; Nishikawa, M.; Mori, T.; Takeya, J.; Shrestha, L. K.; Hill, J. P. Self-assembly as a key player for materials nanoarchitectonics. *Sci. Technol. Adv. Mater.* **2019**, *20*, 51−95.

(4) Akram, B.; Wang, X. Self-Assembly of Ultrathin Nanocrystals to Multidimensional Superstructures. *Langmuir* **2019**, *35*, 10246−10266.

(5) Grzelczak, M.; Marzán, L.; Klajn, R. Stimuli-responsive self-assembly of NP. *Chem. Soc. Rev.* **2019**, *48*, 1342−13361.

(6) Upadhyay, A.; Behara, D.; Sharma, G.; Pala, R.; Sivakumar, S. Self-Directed Assembly of Nanoparticles. A Review on Various Approaches. In *Advanced Theranostic Materials*; Scrivener Publishing LLC: 2015; pp 297−335.

(7) Gao, S.; Song, S.; Wang, J.; Mei, S.; Yuan, J.; Liu, G.; Pana, M. Self-assembled heteromorphous raspberry-like colloidal particles from Pickering-like emulsion polymerization. *Colloids Surf., A* **2019**, *577*, 360−369.

(8) Belbekhouche, S.; Bousserrhine, N.; Alphonse, V.; Floch, F. L.; Mechiche, Y. C.; Menidjel, I.; Carbonnier, B. Chitosan based self-

assembled nanocapsules as antibacterial agent. *Colloids Surf., B* **2019**, *181*, 158−165.
(9) Meng, L.; Chen, W.; Tan, Y.; Zou, L.; Chen, C. P.; Zhou, H. P.; Peng, Q.; Li, Y. D. Fe_3O_4 octahedral colloidal crystals. *Nano Res.* **2011**, *4*, 370.
(10) Zhu, L.; Shan, S.; Petkov, V.; Hu, W.; Kroner, A.; Zheng, J.; Yu, C.; Zhang, N.; Li, Y.; Luque, R.; et al. Ruthenium−nickel−nickel hydroxide nanoparticles for room temperature catalytic hydrogenation. *J. Mater. Chem. A* **2017**, *5*, 7869−787.
(11) Zhu, L.; Jiang, Y.; Zheng, J.; Zhang, N.; Yu, C.; Li, Y.; Pao, C. W.; Chen, J. L.; Jin, C.; Lee, J. F.; et al. Ultrafine Nanoparticle-Supported Ru Nanoclusters with Ultrahigh Catalytic Activity. *Small* **2015**, *11*, 4385−4393.
(12) Zhu, L.; Yang, Z.; Zheng, J.; Hu, W.; Zhang, N.; Li, Y.; Zhong, C.-J.; Ye, H.; Chen, B. H. Decoration of Co/Co3O4 nanoparticles with Ru nanoclusters: a new strategy for design of highly active hydrogenation. *J. Mater. Chem. A* **2015**, *3*, 11716−11719.
(13) Zhang, Y.; Luo, H. Q.; Li, N. B. Hydrogen peroxide sensor based on Prussian blue electrodeposited on (3-mercaptopropyl)-trimethoxysilane polymer-modified gold electrode. *Bioprocess Biosyst. Eng.* **2011**, *34*, 215−221.
(14) Cai, M.; Ho, M.; Pemberton, J. E. Surface Vibrational Spectroscopy of Alkylsilane Layers Covalently Bonded to Monolayers of (3-Mercaptopropyl)trimethoxysilane on Ag Substrates. *Langmuir* **2000**, *16*, 3446−3453.
(15) Zhang, L.; Qi, K. The Fabrication of an Amperometric Immunosensor Based on Double-Layer 2D-Network (3-Mercaptopropyl)trimethoxysilane Polymer and Platinum-Prussian Blue Hybrid Film. *Bull. Chem. Soc. Jpn.* **2018**, *91*, 368−374.
(16) Cui, C.; Li, X.; Liu, J.; Hou, Y.; Zhao, Y.; Zhong, G. Synthesis and functions of Ag_2Snanostructures. *Nanoscale Res. Lett.* **2015**, *10*, No. 431.
(17) Perepelitsa, A. S.; Smirnov, M. S.; Ovchinnikov, O. V.; Latyshev, A. N.; Kotko, A. S. Thermostimulated luminescence of colloidal Ag_2S quantum dots. *J. Lumin.* **2018**, *198*, 357−363.
(18) Robinson, D. A.; White, H. S. Electrochemical Synthesis of Individual Core@Shell and Hollow Ag/Ag2S NP. *Nano Lett.* **2019**, *19*, 5612−5619.
(19) Cai, M.; Ding, C.; Cao, X.; Wang, F.; Zhang, C.; Xian, Y. Label-free fluorometric assay for cytochrome c in apoptotic cells based on near infrared Ag2S quantum dots. *Anal. Chim. Acta* **2019**, *1056*, 153−160.
(20) Chen, G.; Tian, F.; Zhang, Y.; Zhang, Y.; Li, C.; Wang, Q. Tracking of Transplanted Human Mesenchymal Stem Cells in Living Mice using Near-Infrared Ag_2S Quantum Dots. *Adv. Funct. Mater.* **2014**, *24*, 2481−2488.
(21) Shen, Y.; Lifante, J.; Ximendes, E.; Santos, H.; Ruiz, D.; Juárez, B. H.; Gutiérrez, I. Z.; Vera, V. T.; Retama, J. R.; Rosal, E. M.; et al. Perspectives for Ag_2S NIR-II NP in biomedicine: from imaging to multifunctionality. *Nanoscale* **2019**, *11*, 19251−19264.
(22) Jang, J.; Cho, K.; Lee, S. H.; Kim, S. Synthesis and electrical characteristics of Ag2S nanocrystals. *Mater. Lett.* **2008**, *62*, 1438−1440.
(23) Kumari, P.; Chandran, P.; Khan, S. S. Synthesis and characterization of silver sulfide NP for photocatalytic and antimicrobial applications. *J. Photochem. Photobiol., B* **2014**, *141*, 235−240.
(24) Wang, M.; Wang, Y.; Tang, A.; Li, X.; Hou, Y.; Teng, F. Optical properties and self-assembly of Ag_2S NP synthesized by a one-pot method. *Mater. Lett.* **2012**, *88*, 108−111.
(25) Zheng, C.; Qi, Z.; Chen, G. Silver sulfide quantum dots as sensitizer in self-cleaning of Bombyx morisilk fabrics with nano-titania. *J. Text. Inst.* **2016**, *107*, 1501−1510.
(26) Rempel, S. V.; Aleksandrova, N. N.; Kuznetsova, Yu. V.; Gerasimov, E. Yu. Influence of the size and charge of non-stoichiometric silver sulfide NP on their interaction with blood cells. *Inorg. Mater.* **2016**, *52*, 101−105.
(27) Rempel, S. V.; Kuznetsova, Y. V.; Gerasimov, E. Y.; Rempel, A. A. The irradiation influence on the properties of silver sulfide (Ag_2S) colloidal NP. *Phys. Solid State* **2017**, *59*, 1629−1636.
(28) Rempel, S. V.; Kuznetsova, Y. V.; Rempel, A. A. Reduction of colloidal Ag_2S to binary $Ag_{2-x}S$/Ag NP under irradiation in UV and visible range. *Mendeleev Commun.* **2018**, *28*, 96−98.
(29) Li, P.; Peng, Q.; Li, Y. Controlled Synthesis and Self-Assembly of Highly Monodisperse Ag and Ag_2S Nanocrystals. *Chem. - Eur. J.* **2011**, *17*, 941−946.
(30) Tang, A.; Wang, Y.; Ye, H.; Zhou, C.; Yang, C.; Li, X.; Peng, H.; Zhang, F.; Hou, Y.; Teng, F. Controllable synthesis of silver and silver sulfide nanocrystals via selective cleavage of chemical bonds. *Nanotechnology* **2013**, *24*, No. 355602.
(31) Liu, S.; Tao, H.; Liu, Q.; Xu, Z.; Liu, Q.; Luo, J.-L. Rational Design of Silver Sulfide Nanowires for Efficient CO_2 Electroreduction in Ionic Liquid. *ACS Catal.* **2018**, *8*, 1469−1475.
(32) Kuznetsova, Y. V.; Rempel, S. V.; Popov Gerasimov, I. D.; Yu, E.; Rempel, A. A. Stabilization of Ag_2S NP in aqueous solution by MPS. *Colloids Surf., A* **2017**, *520*, 369−377.
(33) Balyakin, I. A.; Rempel, S. V.; Kuznetsova, Yu. V.; Sergeev, A. V.; Rempel, A. A. In *Selforganization of NP in the System of Silver-sulfide-mercaptopropylsilane*, AIP Conference Proceedings, 2017, vol *1886*, p 020002 (https://doi.org/10.1063/1.5002899).
(34) Gorbachev, V. V. *Semiconductor Compounds*; Metallurgy: Moscow, 1980; p 132 (in Russian).
(35) Wu, X. M.; Redmond, P. L.; Liu, H. T.; Chen, Y. H.; Steigerwald, M.; Brus, L. Photovoltage Mechanism for Room Light Conversion of Citrate Stabilized Silver Nanocrystal Seeds to Large Nanoprisms. *J. Am. Chem. Soc.* **2008**, *130*, 9500.

https://dx.doi.org/10.1021/acsomega.0c01994
ACS Omega 2020, 5, 16826−16832